Cellular/Molecular

Organization and Regulation of Small Conductance Ca^{2+}-activated K^+ Channel Multiprotein Complexes

Duane Allen,[3] Bernd Fakler,[1] James Maylie,[2] and John P. Adelman[3]

[1]Department of Physiology, University of Freiburg, Freiburg 09599, Germany, and [2]Department of Obstetrics and Gynecology, and [3]Vollum Institute, Oregon Health and Science University, Portland, Oregon 97329

Small conductance Ca^{2+}-activated K^+ channels (SK channels) are complexes of four α pore-forming subunits each bound by calmodulin (CaM) that mediate Ca^{2+} gating. Proteomic analysis indicated that SK2 channels also bind protein kinase CK2 (CK2) and protein phosphatase 2A (PP2A). Coexpression of SK2 with the CaM phosphorylation surrogate CaM(T80D) suggested that the apparent Ca^{2+} sensitivity of SK2 channels is reduced by CK2 phosphorylation of SK2-bound CaM. By using 4,5,6,7-tetrabromo-2-azabenzimidazole, a CK2-specific inhibitor, we confirmed that SK2 channels coassemble with CK2. PP2A also binds to SK2 channels and counterbalances the effects of CK2, as shown by coexpression of a dominant-negative mutant PP2A as well as a mutant SK2 channel no longer able to bind PP2A. *In vitro* binding studies have revealed interactions between the N and C termini of the channel subunits as well as interactions among CK2 α and β subunits, PP2A, and distinct domains of the channel. In the channel complex, lysine residue 121 within the N-terminal domain of the channel activates SK2-bound CK2, and phosphorylation of CaM is state dependent, occurring only when the channels are closed. The effects of CK2 and PP2A indicate that native SK2 channels are multiprotein complexes that contain constitutively associated CaM, both subunits of CK2, and at least two different subunits of PP2A. The results also show that the Ca^{2+} sensitivity of SK2 channels is regulated in a dynamic manner, directly through CK2 and PP2A, and indirectly by Ca^{2+} itself via the state dependence of CaM phosphorylation by CK2.

Key words: **SK channels; microdomain; kinase; phosphatase; state dependence; regulation**

Introduction

In various neurons, SK channels influence somatic excitability by contributing to afterhyperpolarization (Stocker et al., 1999; Abel et al., 2004), modulate synaptic plasticity by coupling to NMDA receptors (Stackman et al., 2002; Faber et al., 2005; Ngo-Anh et al., 2005), and influence dendritic Ca^{2+} levels (Cai et al., 2004). By exerting a repolarizing conductance in response to increased intracellular Ca^{2+}, SK channels effectively form a Ca^{2+}-mediated feedback loop with their Ca^{2+} sources.

Three homologous SK channels, SK1–3, are expressed in the CNS, exhibiting overlapping yet distinct spatial profiles (Stocker et al., 1999). SK channels are gated solely by intracellular Ca^{2+} ions, show very similar sensitivities to Ca^{2+} (EC_{50} values of ~0.3–0.5 μM) (Köhler et al., 1996), and share a common Ca^{2+}-gating mechanism. Calmodulin (CaM) is constitutively bound to a domain in the proximal region of the intracellular C terminus, the CaM binding domain (CaMBD). Each of the four SK subunits harbors a bound CaM, and binding of Ca^{2+} ions to the N-lobe E–F hands of CaM initiates a conformational rearrangement that results in channel gating (Xia et al., 1998; Keen et al., 1999; Schumacher et al., 2001). Thus, the structure and function of SK channel Ca^{2+}-gating are highly conserved, and all three SK channels expressed in brain show almost identical Ca^{2+} sensitivities.

Despite their similar gating mechanisms, the SK channels appear to serve distinct physiological roles. For example, SK2 channels are largely postsynaptic, whereas at least some SK3 channels are presynaptically located (Roncarati et al., 2001; Obermair et al., 2003; Sailer et al., 2004; Ngo-Anh et al., 2005). Consistent with distinct roles, disruption of any one of the SK genes does not result in altered expression levels of the other, intact genes (Bond et al., 2004). Nevertheless, heteromeric channels have been detected (Strassmaier et al., 2005), and overlapping functions cannot be discounted. Their central role in modulating local Ca^{2+} transients and Ca^{2+}-dependent events suggested that Ca^{2+}-independent signaling mechanisms might modulate SK channels, perhaps by tuning their Ca^{2+} sensitivity. Indeed, a proteomics approach identified CK2 and PP2A as SK2 binding proteins. In *in vitro* assays, CK2 did not phosphorylate the SK2 CaMBD but did phosphorylate CaM in complex with the SK2 CaMBD. Subsequent functional analysis showed that coexpression of SK2 channels with a CaM mutant that contained the phosphorylation surrogate, aspartate (D), at the CK2 phosphorylation substrate site, T80 [CaM(T80D)], resulted in a reduction in the steady-state Ca^{2+} sensitivity of SK2 channels and speeded channel deactivation compared with SK2 coexpression with CaM(T80A) (Bildl et al., 2004). By using native wild-type CaM, CK2, and expressed SK2 channels, we showed that both CK2 and PP2A are associated

Received Aug. 17, 2006; revised Jan. 25, 2007; accepted Jan. 26, 2007.

This work was supported by a National Research Service Award to D.A., National Institutes of Health grants to J.M. and J.P.A., and a grant from the Deutsche Forschungsgemeinschaft to B.F.

Correspondence should be addressed to Dr. John P. Adelman, Vollum Institute, Oregon Health and Science University, 3181 SW Sam Jackson Park Road, Portland, OR 97329. E-mail: adelman@ohsu.edu.

DOI:10.1523/JNEUROSCI.3565-06.2007

 0270-6474/07/272369-08$15.00/0

with expressed SK2 channels and provide opposing regulatory activities. In addition, there are multiple points of interaction between the different proteins, as well as interactions between the N- and C-terminal domains of SK2. Furthermore, CK2 activity toward SK2-associated CaM is state dependent and is controlled by a specific lysine adjacent to one of the CK2–SK2 interaction domains.

Materials and Methods

Molecular biology. Constructs were subcloned into the vector pJPA that contains the cytomegalovirus promoter for protein expression in transfected cells. To generate glutathione *S*-transferase (GST)-fusion proteins, constructs were subcloned into pGEX-4T2 or pGEX-KG (Amersham Biosciences, Piscataway, NJ) expression vectors. To generate N-terminal 6xHis fusion proteins, constructs were subcloned into the vectors pET16b or pET33b (EMD Biosciences, La Jolla, CA). The short form of CK2α (1–340) was used to create the N-terminally His-tagged CK2α. Full-length proteins were used for all other His-tagged fusion proteins. Site-directed mutagenesis was performed with *Pfu* turbo DNA polymerase (Stratagene, La Jolla, CA). All sequences were verified by DNA sequence analysis. Protein expression vectors were transformed into BL-21 (DE3) codon+ *Escherichia coli* (Stratagene) before induction with isopropyl β-D-1-thiogalactopyranoside.

GST pull-down assays. GST agarose beads (Sigma, St. Louis, MO) were resuspended according to the manufacturer's suggested protocol, and 250 μl of slurry was used per reaction. Beads were washed one time with 1 ml of pull-down wash buffer (PWB) [20 mM HEPES, pH 7.8, 10% glycerol, 100 mM KCl, 0.1 mM EDTA, 0.1 mM dithiothreitol (DTT), 0.1% Igepal CA-630 (Sigma)] and then incubated at 4°C for 2 h with ~100 μl of crude-bacterial lysate containing the GST-fusion protein. Lysate was the soluble fraction generated by French pressing 1 L of isopropyl β-D-1-thiogalactopyranoside-induced bacterial culture that had been pelleted and resuspended in 20 ml of 20 mM HEPES buffer, pH 7.8, 1 mM DTT, and complete protease inhibitor mixture tablets (Roche, Mannheim, Germany). Bead–protein complexes were washed one time with 1 ml of PWB followed by a 5 min wash at 4°C with 1 ml of PWB plus 0.1% BSA to prevent nonspecific binding. This was followed by two 1 min washes with 1 ml of PWB. These "baits" were then exposed to an excess (~250 μl) of 6xHis-tagged "prey" protein added as crude-bacterial lysate, and reaction volume was increased to 1 ml with PWB. Bait and prey were incubated together at 4°C overnight, washed four times with 1 ml of PWB, added to 2× protein loading buffer containing 100 mM Tris-Cl, pH 6.8, 100 mM DTT, 4% SDS, 0.2% bromophenol blue, and 20% glycerol, heated to 95°C for 5 min, and run on SDS-PAGE gels. Western blots were prepared from the gels, and specifically retained prey proteins were identified with an anti-6xHis horseradish peroxidase-coupled monoclonal antibody (Clontech, Mountain View, CA).

Electrophysiology. Chinese hamster ovary (CHO) cells were grown in F-12 media supplemented with penicillin–streptomycin and 10% heat-inactivated fetal bovine serum (Invitrogen, Carlsbad, CA). Cells were transfected with pJPA expression plasmids and pEGFP-N1 (Clontech) in a ratio of 10:1 by using Lipofectamine 2000 (Invitrogen). Recordings were performed at room temperature 1–2 d after transfection. Transfected cells were identified by enhanced green fluorescent protein. When filled, pipettes prepared from thin-walled borosilicate glass (World Precision Instruments, Sarasota, FL) had resistances of 2–3 MΩ. For excised patch recordings, the pipette solution contained (in mM): 140 KCl, 10 HEPES, 1.0 EGTA; pH was adjusted to 7.2 with KOH. As calculated according to Fabiato and Fabiato (1979), 0.9943 mM total Ca^{2+} (as $CaCl_2{\cdot}2H_2O$) was added to give 10 μM free Ca^{2+}. Excised patches were superfused with an identical solution or one that contained no calcium with an RSC-200 rapid solution exchanger (Molecular Kinetics, Pullman, WA). Currents were measured at −80 mV and digitized with an EPC9 patch-clamp amplifier (HEKA Elektronik, Lambrecht/Pfalz, Germany). Currents were sampled at 1 kHz and filtered at one-third the sample frequency, and analysis was performed with Pulse (HEKA Elektronik) and Igor (Wavemetrics, Lake Oswego, OR) software. Leak and background currents were measured by changing the bath solution on the inside face of the patch to 0 Ca^{2+} to close SK2 channels. MgATP was applied at a concentration of 5 mM for 2.5 min in the absence of Ca^{2+}, unless stated otherwise.

CK2 activation assay. Protein kinase CK2 assays were performed according to the manufacturer's suggested protocol for the CK2 assay kit (Upstate Biotechnology, Lake Placid, NY). Recombinant, human CK2 was obtained from EMD Biosciences and used at a dilution of 1:20,000.

CK2 phosphorylation assay. Assays were performed as described previously (Bildl et al., 2004). Briefly, purified CaM (2.5 μg) or CaMBD–CaM complex (5 μg) was incubated for 2 h at 30°C in a 50 μl reaction mixture containing 50 mM Tris, pH 7.5, 10 mM MgCl2, 1 μM poly-L-lysine (30–70 kDa; Sigma), 200 μM ATP, 20 μCi/ml [γ-^{32}P] ATP (PerkinElmer, Boston, MA), 1 KU/ml CK2 (human, recombinant, *E. coli*; EMD Biosciences), and 1 mM EGTA, 10 μM Ca^{2+}, or 100 μM Ca^{2+}. Then, 2× protein sample buffer containing 100 μM DTT and 1 mM EGTA was added to the reactions. The samples were heated to 95°C for 5 min and run on 18% PAGE gels. Gels were exposed to a phosphoimager, and densitometry was performed on the images with ImageJ (NIH). The densitometry data contained 21 points in each of the experiments presented; thus, 19 df exist and present a target correlation coefficient of 0.433. For the experiment with poly-L-lysine as the CK2 activator, $r = 0.77$; thus $p < 0.001$. For the experiment, with the SK2 N terminus as the CK2 activator, $r = 0.53$; thus $p < 0.05$. Consequently, all the data presented were within the linear range.

Pharmacology. 4,5,6,7-Tetrabromo-2-azabenzimidazole (TBB) was obtained from EMD Biosciences and used at a concentration of 10 μM.

Data analysis. To determine deactivation time constants, the equation $I_{base} + (I_m - I_{base})e^{-t/\tau}$off was used. For Ca^{2+} concentration–response experiments, each data point represents the average of three sweeps with the 0 Ca^{2+} background current subtracted. The channel was maximally activated by 10 μM Ca^{2+} in all cases. Data points were normalized to the maximum response in 10 μM Ca^{2+}, and the concentration–response data for individual patches were fit with the logistic equation $1/(1 + (EC_{50}/Ca^{2+})^n)$ and forced through 1 to derive an EC_{50} value and hill number for each patch. The EC_{50} values were averaged for all patches for each condition to obtain an average $EC_{50} \pm$ SEM. For display purposes, those concentration–response data from each patch were normalized to 1, and the responses from patches for each condition were averaged to give mean ± SEM for each concentration. The logistic equation was then fit to the average concentration–response as displayed for visualization.

All values are reported as the mean ± SEM of *n* experiments. Statistical significance was evaluated with a Student's *t* test or ANOVA, and $p <$ 0.05 was considered significant.

Results

Heterologous expression studies with surrogates for phosphorylation or dephosphorylation of CK2 phosphorylation sites on CaM suggested that endogenous CK2 phosphorylates SK2-associated CaM at position T80, resulting in a rightward shift of the apparent steady-state Ca^{2+} sensitivity of the channels and faster channel deactivation (Bildl et al., 2004). To directly examine protein kinase activity that coassembled with SK2 channels and to verify the identity as CK2, SK2 channels were expressed in CHO cells, relying on endogenous CaM and CK2 to coassemble into SK2 channel complexes. Rapid solution exchange (~2 ms; see Materials and Methods) was used to examine the deactivation kinetics of the channels. Steady-state currents were evoked by application of 10 μM free Ca^{2+} in the bath solution (see Materials and Methods). On switching from 10 μM free Ca^{2+} to 0 Ca^{2+}, channel deactivation was described by a single exponential with a time constant of 54 ± 2 ms ($n = 10$) (Fig. 1*b*). To activate protein kinase associated with the SK2 channels, patches were exposed to normal 0 Ca^{2+} bath solution with 5 mM MgATP for 2.5 min. Patches were then exposed to 10 μM Ca^{2+} in the absence of MgATP to evoke a steady-state current before deactivation was examined by switching to 0 Ca^{2+} solution. The deactivation rate was significantly increased after MgATP treatment, becoming

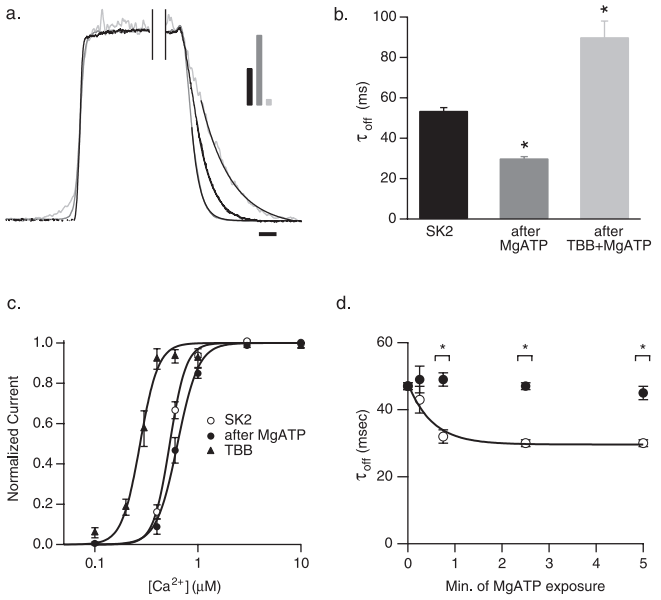

Figure 1. Activation of CK2 speeds SK2 channel deactivation and reduces the apparent Ca^{2+} sensitivity. ***a***, Deactivation of normalized SK2 currents after rapid solution exchange from 10 μM to 0 Ca^{2+}; black trace, control (τ_{off} = 57.0 ms); dark gray trace, after a 2.5 min exposure to 5 mM MgATP in 0 Ca^{2+} (τ_{off} = 29.3 ms); light gray trace, after 2.5 min exposure to 5 mM MgATP in 0 Ca^{2+} and TBB (τ_{off} = 112.4 ms). Single exponential fits are added to traces. Bars in inset indicate relative current amplitudes. Calibration, 50 ms. ***b***, Average SK2 deactivation time constants derived from single exponential fits for the indicated conditions. ***c***, Normalized steady-state Ca^{2+} dose–response relationships for SK2 control (open circle), after application of MgATP (closed circle), and additionally in the presence of TBB (triangle). ***d***, Time course of MgATP effect. Separate groups of patches were exposed to 5 mM MgATP for 0 min (n = 10), 0.25 min (n = 11), 0.75 min (n = 12), 2.5 min (n = 11), or 5 min (n = 8) to generate paired, before (black circles) and after (open circles) time points. The time constant of MgATP effect = 0.5 s.

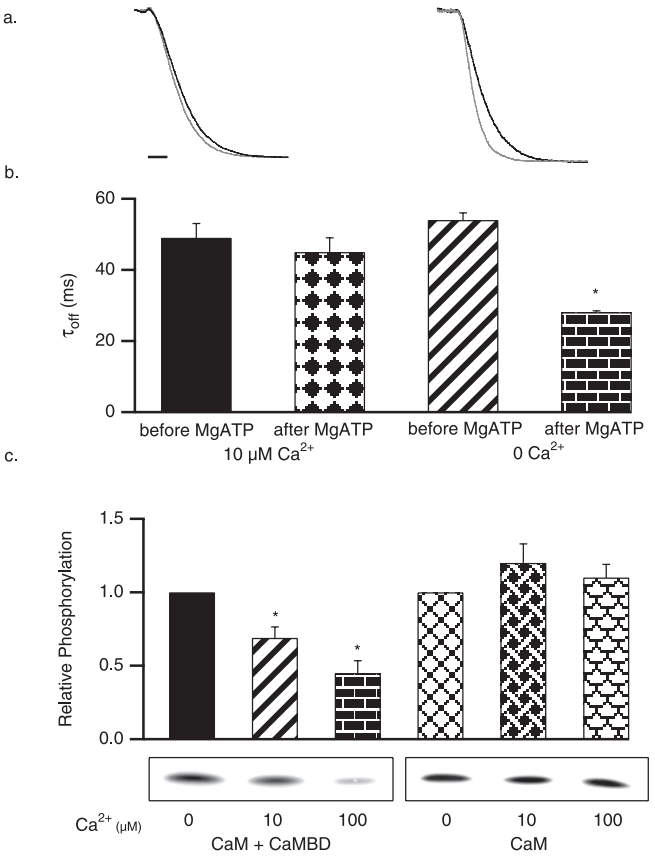

Figure 2. CK2 activity for SK2-associated CaM is state dependent. SK2 current deactivation as in Figure 1, for control SK2 (black trace) and after application of 5 mM MgATP (gray trace; 45 s) in the presence of 10 μM (left) or 0 Ca^{2+} (right). Calibration, 50 ms. ***b***, Average SK2 deactivation time constants derived from single exponential fits for the indicated conditions. ***c***, *In vitro* CK2 phosphorylation reactions, stimulated by poly-L-lysine. Autoradiograph of phosphorylated CaM shows representative results for the conditions indicated, and the bar graph shows the average relative phosphorylation of CaM.

30.0 ± 0.9 ms (n = 6) (Fig. 1*b*). Consistent with these results, steady-state Ca^{2+} dose–response experiments showed that, after protein kinase activation, the apparent EC_{50} value was shifted from 0.53 ± 0.02 μM (Hill coefficient = 6.0 ± 0.2; n = 15) in control to 0.66 ± 0.03 μM (Hill coefficient = 5.5 ± 0.3; n = 15) (Fig. 1*c*). The Hill coefficient was not significantly changed by the addition of MgATP. To determine whether the activated kinase was CK2, the specific inhibitor TBB (10 μM) (Sarno et al., 2001) was coapplied to the patches with MgATP in 0 Ca^{2+} for 2.5 min, and deactivation kinetics were reexamined in the continued presence of TBB. Channel deactivation was significantly slowed by TBB, with a time constant of 94 ± 8 ms (n = 9) (Fig. 1*b*). Consistent with this result, steady-state Ca^{2+} dose–response experiments in the presence of TBB showed an apparent EC_{50} value of 0.28 ± 0.02 μM (Hill coefficient = 7.1 ± 0.3; n = 9) (Fig. 1*c*). The Hill coefficient was significantly changed by the application of TBB ($p < 0.01$; t test).

CK2 phosphorylation of SK2-associated CaM is state dependent

To determine whether the activity of CK2 toward SK2-associated CaM was state dependent, MgATP was applied to patches in the presence of 10 μM Ca^{2+} (open channels) or 0 Ca^{2+} (closed channels). Activation of CK2 while the channels were open did not result in a shift of the deactivation time constant (49 ± 4 ms before MgATP; 45 ± 4 ms after MgATP; n = 6) (Fig. 2*a*,*b*). In contrast, CK2 activation while the channels were closed decreased the deactivation time constant from 54 ± 2 ms before MgATP to 28.1 ± 0.4 ms after MgATP (n = 6) (Fig. 2*a*,*b*). *In vitro* radiolabeled CK2 phosphorylation reactions were performed with either CaM alone or CaM in complex with the CaMBD as substrates. CK2 requires positively charged molecules to phosphorylate CaM (Meggio et al., 1987, 1992); therefore, reactions were stimulated by poly-L-lysine (1 μM) and were performed in the absence or presence of Ca^{2+} (0, 10, or 100 μM). In the absence of Ca^{2+}, CaM was efficiently phosphorylated whether or not it was in complex with the CaMBD. In the presence of Ca^{2+}, CaM alone was phosphorylated equally efficiently, whereas CK2 phosphorylation of CaM in complex with the CaMBD was inhibited, being decreased by 31 ± 6% in 10 μM Ca^{2+} and 55 ± 6% in 100 μM Ca^{2+} (n = 7) (Fig. 2*c*). Together, these results show that CK2 phosphorylates SK2-associated CaM only while the channels are closed.

PP2A is a component of the SK2 channel complex

In the experiments described above, activation of SK2-associated CK2 significantly accelerated channel deactivation, but the time constant was not reduced as much as when SK2 was coexpressed with the CaM phosphorylation surrogate CaMT80D (13.7 ± 0.8 ms; n = 12) (Fig. 3*c*). Moreover, the deactivation time constant measured after application of the CK2 inhibitor TBB (94 ± 5 ms) was much larger than the time constant measured from coexpression of SK2 with the CaM dephosphorylation surrogate CaMT80A (45 ± 1 ms; n = 8; data not shown). Together, the

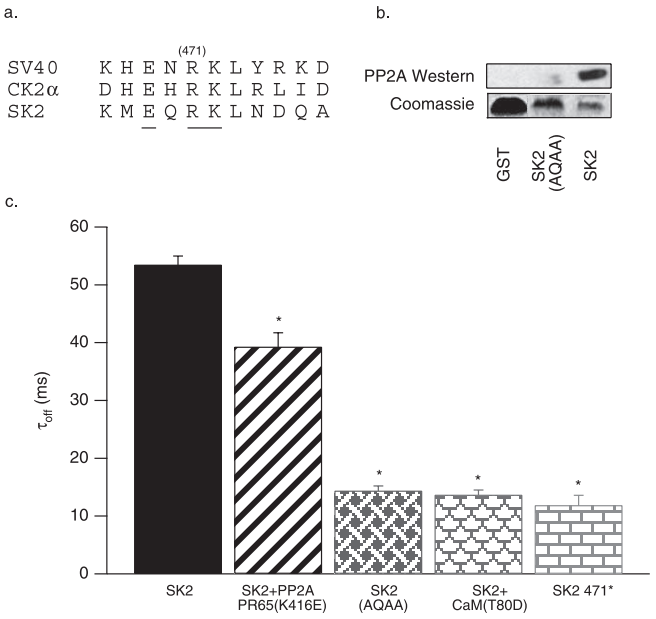

Figure 3. PP2A is coassembled with SK2 channels. ***a***, Amino acid sequence comparison of PP2A binding sites on SV40 small T-antigen, CK2α, and SK2 (467–476). Mutated residues are underlined, and the position of the truncation, R471, is indicated. ***b***, Top, Anti-His Western blot of proteins eluted from GST pull-down experiments with His-tagged PP2A PR65 as prey with the following baits: GST, SK2 396-end containing the mutation EQRK to AQAA, and SK2 396-end. Bottom, Coomassie blue-stained gel showing the input GST-fusion bait proteins. ***c***, Average deactivation time constants derived from single exponential fits for control SK2, SK2 coexpressed with the dominant-negative PP2A (PR65 K416E), the SK2 EQRK to AQAA triple mutant, SK2 coexpressed with CaM T80D, and the SK2 truncation at position 471.

results suggested the presence of a phosphatase activity associated with SK2 channels. Indeed, one of the binding partners isolated with the SK2 C terminus as bait was PP2A (Bildl et al., 2004).

To test for PP2A activity toward SK2, the PP2A dominant-negative mutant K416E in PR65/A, the scaffolding subunit of PP2A, was coexpressed with SK2 channels. This previously described mutation decreases the affinity of PR65/A for the catalytic subunit of PP2A by ~100-fold (Turowski et al., 1997). Consistent with an effect of PP2A on SK2, the deactivation time constant was 39 ± 2 ms ($n = 4$) for cells cotransfected with the mutant PP2A, whereas the deactivation time constant from wild-type control cells was significantly larger: 54 ± 2 ms ($n = 6$) (Fig. 3*c*).

Inspection of the C-terminal domain of SK2 revealed a sequence similar to two known PP2A binding sites, one in SV40 small T-antigen and one in protein kinase CK2 (Fig. 3*a*). Mutation of the sequence EHRK to AHAA in CK2α was shown to abolish binding to PP2A (Heriche et al., 1997); therefore, the homologous sequence in the SK2 C-terminal domain, EQRK (amino acids 469–472), was mutated to AQAA. Bacterially expressed GST-fusion proteins of wild-type and AQAA (469–472) mutants were tested in pull-down assays for their ability to bind to His-tagged PP2A PR65/A. Western blots of the eluted proteins with the anti-His antibody showed that the wild-type SK2 C-terminal domain was capable of binding PR65/A, whereas the triple mutant was greatly diminished in its ability to bind PR65/A (Fig. 3*b*). The triple mutant AEAA (469–472) was introduced into full-length SK2 and expressed in CHO cells. The deactivation time constant of AEAA (469–472) was 14.4 ± 0.8 ms ($n = 6$) (Fig. 3*c*), not significantly different from the deactivation time constant measured from patches coexpressing wild-type SK2 and CaMT80D (13.7 ± 0.8 ms; $n = 12$), nor was it different from the time constant measured for a truncation at position 471 (SK2 471*; 11.9 ± 1.7 ms; $n = 6$) (Fig. 3*c*). Together, the results show that SK2 channels are coassembled complexes with PP2A and protein kinase CK2 and that opposing kinase and phosphatase activities modulate the apparent Ca^{2+} sensitivity of the channels.

Interactions between SK2 and CK2

CK2 was isolated as an SK2 binding protein based on its ability to refold onto the isolated intracellular C-terminal domain of the channel. In control experiments, CK2 was also shown to bind to the intracellular N-terminal domain of SK2, suggesting a complex interaction between CK2 and noncontiguous segments of the SK channel subunit (Bildl et al., 2004). This also implied that the N- and C-terminal domains of the SK2 channel might themselves interact. Therefore, the sites of interaction between CK2 α and β subunits and the SK2 N- and C-terminal domains, and interactions between the intracellular domains themselves, were investigated with GST pull-down experiments. GST was fused with a series of overlapping bacterially expressed proteins that span the N-terminal domain of SK2, and these were immobilized on glutathione-agarose beads. A 6xHis tag was fused to the CK2 α and β subunits and to the SK2 N terminus. These prey were exposed to the GST-fusion protein baits. After washes, the proteins were separated by PAGE and probed as Western blots with an anti-6xHis horseradish peroxidase-coupled monoclonal antibody. The results (Fig. 4*a*) showed that the CK2 α and β subunits bound to a fragment encompassing most of the N-terminal domain (2–140). For CK2β this could not be defined further. CK2α additionally bound to fragment 107–129 but did not bind to fragment 107–124, suggesting that 125–129 (RRALF) comprises the N-terminal binding site for CK2α. A similar strategy was used to examine C-terminal interactions. In this case, a segment of the N-terminal domain of the channel (72–129) also served as prey (Fig. 4*b*). Together, the results showed that the N-terminal domain (72–129) interacts with the CaMBD (433–460) and with a segment close to the C terminus of the channel (558–568). CK2 α and β showed similar patterns of interaction with the C-terminal domain, binding to the CaMBD (433–446) and a segment close to the C terminus (558–568).

SK2 K121 activates SK2-associated CK2

CK2 requires positively charged compounds such as poly-L-lysine or spermine to phosphorylate CaM (Meggio et al., 1992), yet in excised patch experiments, CK2 activity required only MgATP to phosphorylate SK2-associated CaM. The N-terminal domain of SK2 contains a cluster of positively charged residues close to the site of interaction with CK2α. Therefore, the N-terminal domain of SK2, residues 2–140, was expressed in bacteria as a GST-fusion, and the isolated protein was used in CK2 activation assays, in the absence of poly-L-lysine. As shown in Figure 5*a*, the N-terminal domain of SK2 significantly enhanced CK2 activity to phosphorylate a prototype CK2 phosphorylation substrate peptide. The N-terminal domain of SK2 was also used to stimulate CK2 activity to phosphorylate CaM, either alone or in complex with the CaMBD, without or with Ca^{2+} present in the reaction. Similar to the results with poly-L-lysine to stimulate CK2 activity (Fig. 2*c*), CaM was efficiently phosphorylated by SK2 N-terminal domain-stimulated CK2 in the absence of Ca^{2+}, whether or not CaM was bound to the CaMBD. The presence of Ca^{2+} did not reduce the efficiency of CaM phosphorylation in the absence of the CaMBD, but when CaM was bound to the CaMBD, Ca^{2+} reduced the efficiency of CK2 phosphorylation by 42 ± 9% in 10 μM and 50 ± 9% in 100 μM (Fig. 5*b*). To further

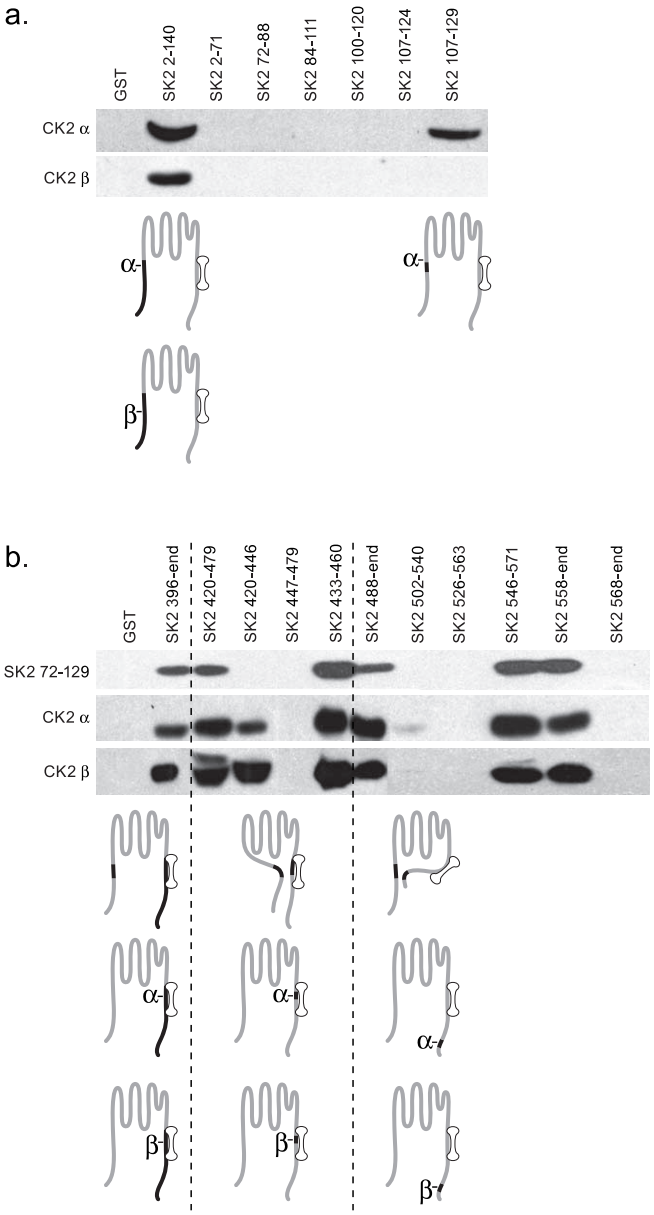

Figure 4. Interactions between domains of SK2 and CK2. ***a***, GST pull-down experiments used the indicated fragments of the N-terminal domain of SK2 as baits to detect interactions with N-terminally His-tagged CK2 α or CK2 β. Specifically bound prey proteins were detected by Western blotting with an anti-His antibody. ***b***, Same as in ***a*** but with GST-fusion proteins of the C-terminal domain of SK2 as baits and additional testing for interactions with the membrane proximal portion of the SK2 N-terminal domain. Subunit schematics represent the interactions detected by the pull-down results.

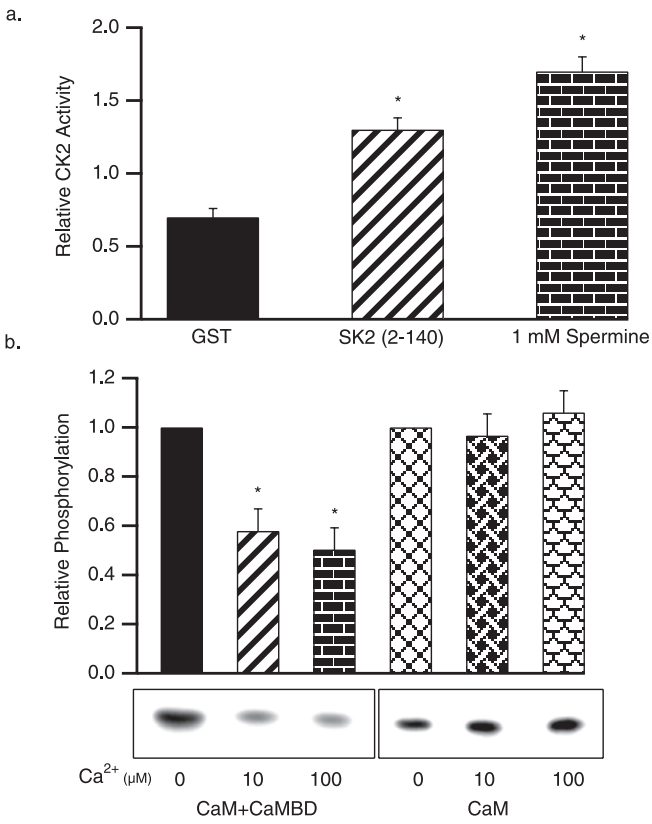

Figure 5. The SK2 N-terminal domain activates CK2. ***a***, Average CK2 phosphorylation of a prototypic CK2 substrate peptide stimulated by control GST, the SK2 N-terminal domain, or spermine. ***b***, *In vitro* CK2 phosphorylation of CaM, either bound to the CaMBD (left) or alone (right), stimulated by the SK2 N-terminal domain. Autoradiograph of phosphorylated CaM shows representative results for the conditions indicated, and the bar graph shows the average relative phosphorylation of CaM.

define the residues responsible for influencing CK2 activity, site-directed mutations were introduced into the SK2 N-terminal domain, replacing positively charged residues with alanine (Fig. 6*a*). The channels were expressed in CHO cells, and the effects of MgATP were evaluated. Only substitution at a single position showed an effect: the point mutation K121A increased the deactivation time constant from 48 ± 2 to 93 ± 4 ms ($n = 10$) and eliminated the effect of MgATP (80 ± 5 ms; $n = 10$) (Fig. 6*b*,*c*). The apparent Ca^{2+} sensitivity of K121A channels was appropriately left-shifted to 0.29 ± 0.3 μM ($n = 6$; data not shown). Although not significant ($p = 0.09$), there was a trend to reduced deactivation time constants with MgATP, suggesting that in the absence of K121, other nearby positive charges may influence the activity of SK2-associated CK2. Therefore, all five proximal lysine residues were simultaneously changed to alanine (SK2 5K to A). In this case, the trend with MgATP application was eliminated (100 ± 2 ms before MgATP; 98 ± 3 ms after MgATP; $n = 6$; $p = 0.58$) (Fig. 6*b*,*c*).

Discussion

The results presented here define CK2 and PP2A as components of native SK2 channel complexes and show that they serve opposing roles in regulating Ca^{2+} gating. The SK2 channel α subunits, CaM, CK2, and PP2A, are intricately arranged, allowing a single lysine residue in the N-terminal domain of SK2 to act as a molecular switch, activating CK2 to phosphorylate SK2-associated CaM only when the channels are closed. Additionally, the present findings identify three discrete points of interaction between the α and β subunits of CK2 and SK2, a 5-amino-acid motif in the membrane-proximal region of the intracellular N terminus, the predicted hinge in the extended "BC" helix of the CaMBD (Keen et al., 1999; Schumacher et al., 2001), and a 10-amino-acid domain close to the C terminus of the channel. PP2A binds to a discrete site on the SK2 subunit, just distal to the CaMBD. The amino acid sequence of the PP2A binding site is similar to the PP2A binding site on CK2a (Heriche et al., 1997), suggesting that there may also be interactions between PP2A and CK2a. The present results redefine the native SK2 channel as a polyprotein complex of 4 channel α subunits, 4 CaM proteins, up to as many as 16 CK2 subunits (4 × $\alpha 2\beta 2$), and 8 PP2A subunits (4 ×

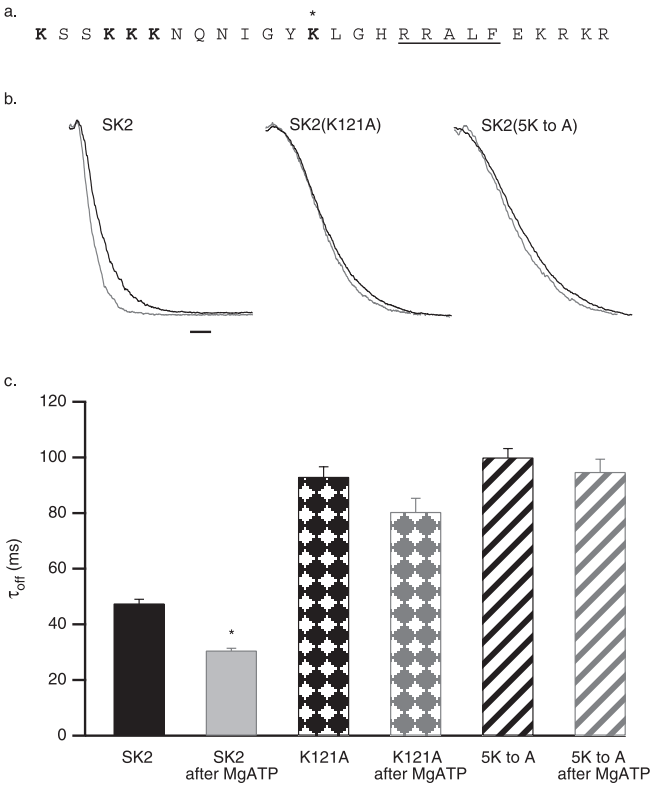

Figure 6. K121 regulates CK2 coassembled with SK2 channels. ***a***, Amino acid sequence (109–134) of the positively charged cluster in the SK2 N-terminal domain that includes the identified CK2 α binding site (RRALF; underlined). Asterisk indicates K121; the mutated lysine residues are in bold type. ***b***, SK2 current deactivation for control SK2 (black traces) and after application of 5 mM MgATP (gray traces) for wild-type, SK2 K121A, and SK2 5KtoA channels. Calibration, 50 ms. ***c***, Average deactivation time constants derived from single exponential fits for SK2, SK2 K121A, and SK2 5KtoA before and after 5 mM ATP application.

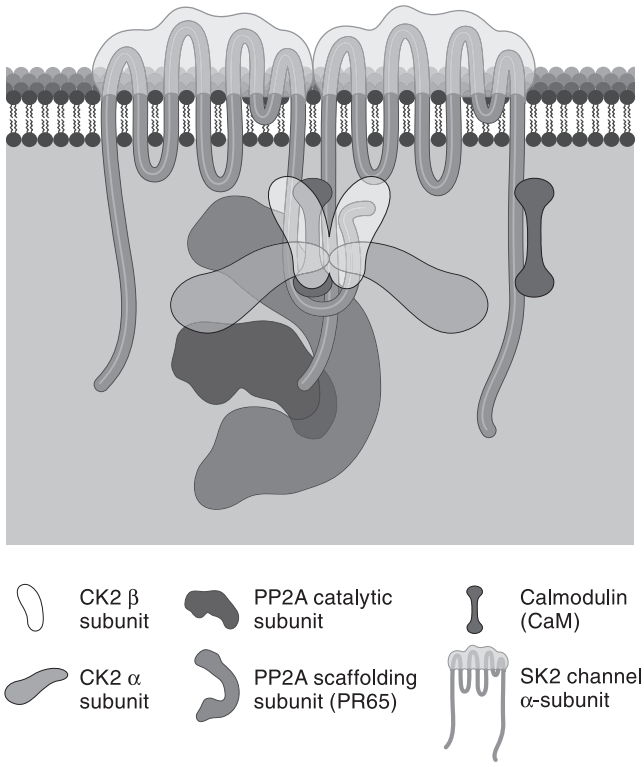

Figure 7. Model for coassembled SK2, CaM, CK2, and PP2A. The model, consistent with pull-down results, represents two of the four SK2 subunits and invokes an intersubunit interaction. CK2 and PP2A are drawn approximately to scale. In this configuration, the N-terminal domain of SK2 that includes K121 is positioned close to CK2 that binds to the adjacent sequence, RRALF.

PP2A/C and PR65/A). Overall, the picture that emerges is one of multiple, and likely state-dependent, overlapping interactions between the various proteins. Further elucidation of this complex will require different approaches, such as x-ray crystallography. In addition, there are interactions between SK2 subunits at intracellular domains. Sequences in the membrane-proximal half of the N-terminal domain interact with the CaMBD and the same 10-amino-acid motif near the C terminus that interacts with CK2α. These results suggest that the N and C termini of the SK2 channel are in close proximity, and the intracellular termini might be physically constrained.

It is not yet clear whether the interactions detected between the different domains of the SK2 subunits reflect intrasubunit or intersubunit interactions. One model that is consistent with the data is presented in Figure 7 and invokes an intersubunit interaction between the C-terminal domain of one SK2 subunit and the N-terminal domain of the adjacent subunit. This configuration brings into spatial proximity sequences that are located distally in the primary amino acid sequence of SK2, and it permits CK2 α and β and PP2A to be positioned to account for their binding patterns. The N-terminal domain of SK2 and both subunits of CK2 interact with two sites in the C terminus. It is possible that these biochemical binding results may reflect different, state-dependent interactions in functional channels.

The CK2 holoenzyme is constitutively active, and, in many cases, basic compounds such as poly-L-lysine stimulate activity. In this regard, CaM stands as a rare exception, such that the holoenzyme is essentially inactive toward CaM but is dramatically stimulated by polybasic peptides (Meggio et al., 1992; Arrigoni et al., 2004), yet application of MgATP to inside-out patches was sufficient to activate CK2 to phosphorylate SK2-associated CaM, and site-directed mutagenesis identified a single lysine residue, K121, as being responsible for SK2-bound CK2 activity. Apparently the intricate arrangement of the multiprotein SK2 complex positions K121 to activate CK2. The model presented in Figure 7 positions the positively charged region of the N terminus, including K121, close to CK2; however, CK2 showed a state dependence in its ability to phosphorylate SK2-associated CaM, being able to phosphorylate channels only in the closed state, suggesting that the different conformations of the protein complex in the open and closed states affect the relative proximity of K121 to CK2. Although this is the most parsimonious explanation for the results, it is also possible that the K121A mutation may otherwise affect CK2 binding. Polybasic compounds stimulate CK2 activity likely through interactions with the acid cluster on the β subunit (Niefind et al., 2001) (but see Lawson et al., 2006). The presence of positive charges may result in charge shielding of the acid loop that normally inhibits CK2 activity (Niefind et al., 2001). In this case, because of the specific conformation, K121 serves as a competent surrogate for poly-L-lysine.

The SK2 channel complex also contains PP2A. Direct binding of PP2A to the SK2 C-terminal domain is required for PP2A function within the SK2 channel complex. This is particularly emphasized by the very rapid deactivation kinetics that are observed in inside-out patches containing SK2 channels that harbor mutations in the PP2A binding site, without previous application of MgATP, suggesting that the channels are fully phosphorylated

before patch excision. In addition to the β regulatory subunit, the scaffolding subunit PR65/A was also identified by a proteomics approach (Bildl et al., 2004). PP2A frequently exists as a heterotrimer composed of PP2A/C, PR65/A, and the β subunit that serves to direct compartmentalization and modify substrate specificity (Sontag, 2001). It may be that the SK2 channel binding domains serve a function similar to the PP2A/B subunit. CK2α and PP2A can also bind to each other (Heriche et al., 1997) and may interact within the SK2 channel complex, although this remains to be shown directly.

Activity of CK2 and PP2A on SK2-associated CaM is regulated indirectly, at least in part, through Ca^{2+}, because kinase activity is state dependent. Interestingly, the model presented in Figure 7 that brings K121 in close proximity to CK2 also positions a cluster of 10 potential phosphorylation substrate sites (556–580 aa) in the C terminus of the channel close to CK2 and K121. It is possible that dynamic introduction and removal of phosphates in this domain create an overall net charge cloud with K121 that tunes the activity of CK2 toward SK2-associated CaM. Although we have emphasized the extreme cases for CK2/PP2A activities in which the channels are fully phosphorylated or dephosphorylated, four CaMs are associated with each SK channel, and the responses to CK2 and PP2A may be graded, reflecting partial phosphorylation. Moreover, the effects of phosphorylation may be different if the phosphorylated CaMs are adjacent to or across from each other in the tetrameric channel. This potential complexity may permit exquisite and dynamic tuning of the apparent Ca^{2+} sensitivities of the channels and may account for the ability to describe deactivation as well as steady-state Ca^{2+} responses of the mixed intermediate states with a single exponential or Hill fit, respectively.

CK2 and PP2A are highly conserved, ubiquitously expressed proteins. CK2 is enriched in brain, particularly the dendritic arbor (Krek et al., 1992; Moreno et al., 1999). In dendritic spines (Faber et al., 2005; Ngo-Anh et al., 2005) and shafts (Cai et al., 2004), SK2 channels form functional Ca^{2+}-mediated feedback loops with their Ca^{2+} sources, NMDA receptors, or voltage-dependent Ca^{2+} channels. The influx of Ca^{2+} through these Ca^{2+} sources activates nearby SK2 channels, exerting a repolarizing influence on the membrane potential that ultimately could lead to an attenuation of Ca^{2+} influx. The state dependence of CK2 activity toward SK2-associated CaM will shape the influence of SK2 channels on excitability and dendritic Ca^{2+} transients. During quiescent periods, such as between bursts of action potentials or EPSPs, CK2 activity will decrease the effective Ca^{2+} sensitivity of the channels and the repolarizing effect of the SK channel on reexposure to Ca^{2+}. With a persistent elevation in Ca^{2+}, such as after frequent action potential discharge or synaptic activity, PP2A activity will likely predominate and SK2 channels will become more sensitive to Ca^{2+}, thus increasing the open probability of the SK2 channels and exerting an increased repolarizing influence. This feedback mechanism between CK2 and PP2A fine-tunes SK2 channels in an activity-dependent manner to dynamically shape local changes in Ca^{2+} levels.

SK2 channels and NMDA receptors are closely positioned in the confined Ca^{2+} signaling domain of dendritic spines, where Ca^{2+} mediates reciprocal interactions between them. Interestingly, both are directly influenced by CaM and CK2, but in opposite directions. For SK channels, CaM mediates Ca^{2+} gating, increasing activity, whereas CK2 phosphorylation of SK2-associated CaM reduces channel activity. For NMDA receptors, CaM mediates Ca^{2+}-induced inactivation (Ehlers et al., 1996; Krupp et al., 1999; Rycroft and Gibb, 2002), whereas CK2 phosphorylation enhances activity (Lieberman and Mody, 1999). Therefore, the activation of CK2 may additively increase the NMDA component of EPSPs, by directly increasing NMDA receptor activity and decreasing the SK-mediated repolarization that favors reblock of NMDA receptors by external Mg^{2+} ions. Indeed, activity-dependent activation of CK2 has been implicated in the processes underlying the induction of long-term potentiation in CA1 neurons (Charriaut-Marlangue et al., 1991). Additionally, CK2 phosphorylation of NR2B interrupts an association with PSD-95 (postsynaptic density-95) and decreases surface expression (Chung et al., 2004). PP2A also associates with NMDA receptors containing the developmentally regulated NR3A subunit and results in dephosphorylation of the PKA substrate site S897 on associated NR1 subunits (Chan and Sucher, 2001; Ma and Sucher, 2004). PP2A has also been implicated in certain forms of metaplasticity (Woo and Nguyen, 2002). Therefore, SK2 channels and NMDA receptors that comprise a discrete, local Ca^{2+} signaling microdomain may be coordinately regulated by associated CK2 and PP2A, thus influencing synaptic strength and plasticity.

References

Abel HJ, Lee JC, Callaway JC, Foehring RC (2004) Relationships between intracellular calcium and afterhyperpolarizations in neocortical pyramidal neurons. J Neurophysiol 91:324–335.

Arrigoni G, Marin O, Pagano MA, Settimo L, Paolin B, Meggio F, Pinna LA (2004) Phosphorylation of calmodulin fragments by protein kinase CK2: mechanistic aspects and structural consequences. Biochemistry 43:12788–12798.

Bildl W, Strassmaier T, Thurm H, Andersen J, Eble S, Oliver D, Knipper M, Mann M, Schulte U, Adelman JP, Fakler B (2004) Protein kinase CK2 is coassembled with small conductance Ca(2+)-activated K^+ channels and regulates channel gating. Neuron 43:847–858.

Bond CT, Herson PS, Strassmaier T, Hammond R, Stackman R, Maylie J, Adelman JP (2004) Small conductance $Ca2^+$-activated K^+ channel knock-out mice reveal the identity of calcium-dependent afterhyperpolarization currents. J Neurosci 24:5301–5306.

Cai X, Liang CW, Muralidharan S, Kao JP, Tang CM, Thompson SM (2004) Unique roles of SK and Kv4.2 potassium channels in dendritic integration. Neuron 44:351–364.

Chan SF, Sucher NJ (2001) An NMDA receptor signaling complex with protein phosphatase 2A. J Neurosci 21:7985–7992.

Charriaut-Marlangue C, Otani S, Creuzet C, Ben-Ari Y, Loeb J (1991) Rapid activation of hippocampal casein kinase II during long-term potentiation. Proc Natl Acad Sci USA 88:10232–10236.

Chung HJ, Huang YH, Lau LF, Huganir RL (2004) Regulation of the NMDA receptor complex and trafficking by activity-dependent phosphorylation of the NR2B subunit PDZ ligand. J Neurosci 24:10248–10259.

Ehlers MD, Zhang S, Bernhardt JP, Huganir RL (1996) Inactivation of NMDA receptors by direct interaction of calmodulin with the NR1 subunit. Cell 84:745–755.

Faber ES, Delaney AJ, Sah P (2005) SK channels regulate excitatory synaptic transmission and plasticity in the lateral amygdala. Nat Neurosci 8:635–641.

Fabiato A, Fabiato F (1979) Calculator programs for computing the composition of the solutions containing multiple metals and ligands for experiments in skinned muscle cells. J Physiol (Lond) 75:463–505.

Heriche JK, Lebrin F, Rabilloud T, Leroy D, Chambaz EM, Goldberg Y (1997) Regulation of protein phosphatase 2A by direct interaction with casein kinase 2alpha. Science 276:952–955.

Keen JE, Khawaled R, Farrens DL, Neelands T, Rivard A, Bond CT, Janowsky A, Fakler B, Adelman JP, Maylie J (1999) Domains responsible for constitutive and Ca(2+)-dependent interactions between calmodulin and small conductance Ca(2+)-activated potassium channels. J Neurosci 19:8830–8838.

Krek W, Maridor G, Nigg EA (1992) Casein kinase II is a predominantly nuclear enzyme. J Cell Biol 116:43–55.

Krupp JJ, Vissel B, Thomas CG, Heinemann SF, Westbrook GL (1999) Interactions of calmodulin and α-actinin with the NR1 subunit modulate

Ca^{2+}-dependent inactivation of NMDA receptors. J Neurosci 19:1165–1178.

Köhler M, Hirschberg B, Bond CT, Kinzie JM, Marrion NV, Maylie J, Adelman JP (1996) Small-conductance, calcium-activated potassium channels from mammalian brain. Science 273:1709–1714.

Lawson K, Larentowicz L, Artim S, Hayes CS, Gilmour SK (2006) A novel protein kinase CK2 substrate indicates CK2 is not directly stimulated by polyamines in vivo. Biochemistry 45:1499–1510.

Lieberman DN, Mody I (1999) Casein kinase-II regulates NMDA channel function in hippocampal neurons. Nat Neurosci 2:125–132.

Ma OK, Sucher NJ (2004) Molecular interaction of NMDA receptor subunit NR3A with protein phosphatase 2A. NeuroReport 15:1447–1450.

Meggio F, Brunati AM, Pinna LA (1987) Polycation-dependent, Ca^{2+}-antagonized phosphorylation of calmodulin by casein kinase-2 and a spleen tyrosine protein kinase. FEBS Lett 215:241–246.

Meggio F, Boldyreff B, Marin O, Marchiori F, Perich JW, Issinger OG, Pinna LA (1992) The effect of polylysine on casein-kinase-2 activity is influenced by both the structure of the protein/peptide substrates and the subunit composition of the enzyme. Eur J Biochem 205:939–945.

Moreno FJ, Diaz-Nido J, Jimenez JS, Avila J (1999) Distribution of CK2, its substrate MAP1B and phosphatases in neuronal cells. Mol Cell Biochem 191:201–205.

Ngo-Anh TJ, Bloodgood BL, Lin M, Sabatini BL, Maylie J, Adelman JP (2005) SK channels and NMDA receptors form a Ca^{2+}-mediated feedback loop in dendritic spines. Nat Neurosci 8:642–649.

Niefind K, Guerra B, Ermakowa I, Issinger OG (2001) Crystal structure of human protein kinase CK2: insights into basic properties of the CK2 holoenzyme. EMBO J 20:5320–5331.

Obermair GJ, Kaufmann WA, Knaus HG, Flucher BE (2003) The small conductance Ca^{2+}-activated K^+ channel SK3 is localized in nerve terminals of excitatory synapses of cultured mouse hippocampal neurons. Eur J Neurosci 17:721–731.

Roncarati R, Di Chio M, Sava A, Terstappen GC, Fumagalli G (2001) Presynaptic localization of the small conductance calcium-activated potassium channel SK3 at the neuromuscular junction. Neuroscience 104:253–262.

Rycroft BK, Gibb AJ (2002) Direct effects of calmodulin on NMDA receptor single-channel gating in rat hippocampal granule cells. J Neurosci 22:8860–8868.

Sailer CA, Kaufmann WA, Marksteiner J, Knaus HG (2004) Comparative immunohistochemical distribution of three small-conductance Ca^{2+}-activated potassium channel subunits, SK1, SK2, and SK3 in mouse brain. Mol Cell Neurosci 26:458–469.

Sarno S, Reddy H, Meggio F, Ruzzene M, Davies SP, Donella-Deana A, Shugar D, Pinna LA (2001) Selectivity of 4,5,6,7-tetrabromobenzotriazole, an ATP site-directed inhibitor of protein kinase CK2 ("casein kinase-2"). FEBS Lett 496:44–48.

Schumacher MA, Rivard AF, Bachinger HP, Adelman JP (2001) Structure of the gating domain of a Ca^{2+}-activated K^+ channel complexed with Ca^{2+}/calmodulin. Nature 410:1120–1124.

Sontag E (2001) Protein phosphatase 2A: the Trojan horse of cellular signaling. Cell Signal 13:7–16.

Stackman RW, Hammond RS, Linardatos E, Gerlach A, Maylie J, Adelman JP, Tzounopoulos T (2002) Small conductance Ca^{2+}-activated K^+ channels modulate synaptic plasticity and memory encoding. J Neurosci 22:10163–10171.

Stocker M, Krause M, Pedarzani P (1999) An apamin-sensitive Ca^{2+}-activated K^+ current hippocampal pyramidal neurons. Proc Natl Acad Sci USA 96:4662–4667.

Strassmaier T, Bond CT, Sailer CA, Knaus HG, Maylie J, Adelman JP (2005) A novel isoform of SK2 assembles with other SK subunits in mouse brain. J Biol Chem 280:21231–21236.

Turowski P, Favre B, Campbell KS, Lamb NJ, Hemmings BA (1997) Modulation of the enzymatic properties of protein phosphatase 2A catalytic subunit by the recombinant 65-EC50a regulatory subunit PR65alpha. Eur J Biochem 248:200–208.

Woo NH, Nguyen PV (2002) "Silent" metaplasticity of the late phase of long-term potentiation requires protein phosphatases. Learn Mem 9:202–213.

Xia X-M, Fakler B, Rivard A, Wayman G, Johnson-Pais T, Keen JE, Ishii T, Hirschberg B, Bond CT, Lutsenko S, Maylie J, Adelman JP (1998) Mechanism of calcium gating in small-conductance calcium-activated potassium channels. Nature 395:503–507.